The Plant Cell, Vol. 9, 1515–1525, September 1997 © 1997 American Society of Plant Physiologists

RESEARCH ARTICLE

Expression of the C_4 *Me1* Gene from *Flaveria bidentis* Requires an Interaction between 5′ and 3′ Sequences

Jerry S. Marshall,[a,1] John D. Stubbs,[b] Julie A. Chitty,[a] Brian Surin,[c] and William C. Taylor[a,c,2]

[a] CSIRO Plant Industry, GPO Box 1600, Canberra 2601, Australia
[b] Department of Biology, San Francisco State University, San Francisco, California 94132
[c] Cooperative Research Centre for Plant Science, GPO Box 475, Canberra 2601, Australia

The efficient functioning of C_4 photosynthesis requires the strict compartmentation of a suite of enzymes in either mesophyll or bundle sheath cells. To determine the mechanism controlling bundle sheath cell–specific expression of the NADP–malic enzyme, we made a set of chimeric constructs using the 5′ and 3′ regions of the *Flaveria bidentis Me1* gene fused to the β-glucuronidase *gusA* reporter gene. The pattern of GUS activity in stably transformed *F. bidentis* plants was analyzed by histochemical and cell separation techniques. We conclude that the 5′ region of *Me1* determines bundle sheath specificity, whereas the 3′ region contains an apparent enhancer-like element that confers high-level expression in leaves. The interaction of 5′ and 3′ sequences was dependent on factors that are present in the C_4 plant but not found in tobacco.

INTRODUCTION

In the C_4 photosynthetic pathway, plants spatially separate the initial fixation and subsequent utilization of CO_2 to avoid the wasteful process of photorespiration. The efficient operation of C_4 photosynthesis requires the strict compartmentation of a number of key enzymes in either mesophyll or bundle sheath cells (Hatch, 1987). This compartmentation in turn relies on cell-specific expression of the genes encoding the enzymes (Furbank and Taylor, 1995). For this reason, C_4 plants provide an attractive system for studying the factors regulating cell-specific gene expression.

In several recent studies, attempts have been made to elucidate the molecular basis of cell-specific expression of various genes required in C_4 photosynthesis. However, because of the lack of a facile transformation system for any C_4 species, these studies have relied on more or less indirect approaches. Transient expression assays of promoter–reporter gene fusions introduced into isolated maize mesophyll protoplasts (Sheen, 1990, 1991) or maize leaf sections (Matsuoka and Numazawa, 1991; Bansal et al., 1992; Bansal and Bogorad, 1993; Viret et al., 1994; Purcell et al., 1995) are among the approaches that have been used. In addition, the expression of reporter genes driven by promoters from C_4 genes has been studied in stably transformed C_3 plants (Matsuoka and Sanada, 1991; Matsuoka et al., 1993, 1994; Stockhaus et al., 1994).

Although much information has been gained from the above-mentioned studies, each of the approaches used has some potential shortcomings. For example, the disturbance caused by isolation of protoplasts and by electroporation or particle bombardment may alter gene expression. In addition, changes in the physical characteristics of leaves during development may affect the penetration of DNA-coated particles into different cell types (Viret et al., 1994). Finally, the analysis of the expression of genes required for C_4 photosynthesis using C_3 plants has obvious limitations. For instance, C_4-specific regulatory factors are unlikely to be present in C_3 plants, thus requiring cautious interpretation of data obtained in such a heterologous system.

To avoid these limitations, we have developed an efficient method for Agrobacterium-mediated stable transformation of the C_4 dicot *Flaveria bidentis* (Chitty et al., 1994). The development of this method has opened the door for the study of factors regulating the cell-specific expression of genes required for C_4 photosynthesis in a homologous C_4 plant. In the work presented here, we used the *F. bidentis Me1* gene, which encodes the isoform of NADP–malic enzyme (NADP-ME) used in C_4 photosynthesis (Marshall et al., 1996), to study the *cis* regulatory elements that lead to high-level, bundle sheath cell–specific expression. We found that both upstream and downstream regions of the *Me1* gene are required to confer the expected expression pattern and that the effects of these

[1] Current address: Cooperative Research Centre for Plant Science, GPO Box 475, Canberra 2601, Australia.
[2] To whom correspondence should be addressed. E-mail bt@pi.csiro.au; fax 61-6-246-5000.

two regions are distinct. Elements located in the upstream region of *Me1* are responsible for bundle sheath preferential expression, whereas elements located downstream of the *Me1* stop codon are required for high-level expression in leaves.

RESULTS

Construction of *Me1–gusA* Chimeric Genes

To determine the role(s) of the regions flanking the *F. bidentis* *Me1* gene in directing the high-level, bundle sheath–specific expression of *Me1*, we made a series of constructs containing the *gusA* reporter gene encoding β-glucuronidase (GUS; Jefferson, 1987). Two constructs contained 2121 bp of DNA upstream of the *Me1* translation start codon plus exon 1 (30 bp), intron 1 (186 bp), and 24 bp of exon 2 fused in-frame to the 5′ end of the *gusA* gene from pKIWI101 (Janssen and Gardner, 1989). In the first construct, termed ME20, the *gusA* gene was followed by the octopine synthase (*ocs*) 3′ terminator, which was also derived from pKIWI101 (Figure 1A). In the second construct (ME29), the *ocs* 3′ terminator was replaced by a 5.9-kb fragment containing the region immediately downstream of the *Me1* translation stop codon (Figure 1B). Assuming the correct excision of intron 1 from *Me1*, both constructs were predicted to encode a chimeric protein containing the first 18 (of an estimated 60) amino acids of the NADP-ME chloroplast transit peptide followed by a single threonine and the entire GUS protein.

Because most plant genes are regulated primarily by sequences at their 5′ ends, we also made a series of constructs containing progressive deletions of upstream sequences from *Me1*. As shown in Figure 1C, the three constructs included all of the *Me1* 5′ untranslated region plus 311, 578, or 1023 bp of upstream DNA fused to *gusA*.

The 3′ Region of *Me1* Is Required for High-Level Expression in Leaves

Sections of leaves taken from greenhouse-grown *F. bidentis* plants transformed with ME20 or ME29 were incubated in a 5-bromo-4-chloro-3-indolyl β-D-glucuronide (X-gluc) solution to allow histochemical determination of the level and pattern of GUS expression conferred by these gene constructs. There were no differences in patterns or levels of staining between primary transformants and their progeny. Figure 2 shows a typical pattern of staining for ME20-transformed plants. Only very faint staining was apparent in leaves, even after prolonged incubation. Because of this very low level of staining, it was not possible to determine histochemically the cell-type distribution of GUS expression in leaves of ME20-transformed plants. Similar results were obtained in plants transformed with ME25, ME26, and ME27 (Figure 1C). These constructs have shorter *Me1* 5′ regions (data not shown). Thus, constructs with only 5′ regions of the *Me1* gene produced very faint or no detectable histochemical staining in leaves.

In contrast, intense blue staining was observed when leaves of ME29-transformed plants were incubated in X-gluc solution for relatively short times. Figure 3A shows a surface view of a typical leaf in which it was evident that the blue color was concentrated around the veins. To determine the cell-type distribution of GUS activity, leaves were sectioned after histochemical staining and examined at higher magnification by using both bright- and dark-field illumination. As shown in Figure 4A, the GUS reaction product was most concentrated in the bundle sheath cells of leaves of ME29-transformed plants. Bundle sheath cells are clearly visible as a tightly organized ring of cells around each vein. Thin sections examined under dark-field illumination provided higher resolution. Figures 4B and 4C also show that GUS was concentrated in bundle sheath cells. Some of the GUS product was observed in mesophyll cells, particularly those adjacent to bundle sheath cells. However, the level of GUS staining observed in mesophyll cells was always significantly lower than that seen in bundle sheath cells, unless X-gluc incubations were performed for extended periods of time. High levels of GUS were also detected in some parts of veins, as shown in Figure 4D, in which one vein was sectioned longitudinally.

Histochemical Determination of GUS Activity in Other Organs

Histochemical GUS staining also was observed in other regions of plants transformed with both ME20 and ME29. As shown in Figures 2 and 3, high levels of GUS were seen in stem sections and in the meristematic regions of shoot apices. The intensity and pattern of this non-leaf-associated staining were similar in plants transformed with either construct. GUS staining in stems and shoot apices was also detected in plants transformed with the 5′ deletion constructs ME25, ME26, and ME27 at levels similar to ME20 and ME29 (data not shown). The dark staining in stems was found in xylem parenchyma cells, in cells of the cambium, and in a layer of parenchyma cells surrounding the outer side of the phloem (Figure 3B). All of these cells contain significant numbers of chloroplasts. Other parenchyma cells containing fewer chloroplasts also showed GUS staining; however, GUS accumulation was lower in these cells. Figure 3C shows a longitudinal section of a shoot tip in which GUS staining is evident in lateral meristematic regions, similar to that seen in Figure 2. (Apical staining was also observed in ME29-transformed material, but it is not visible in this glancing section, which does not pass through the shoot apex.) In Figure 2, additional staining is visible below the apex, but this is due to staining of vascular parenchyma cells as described for stems.

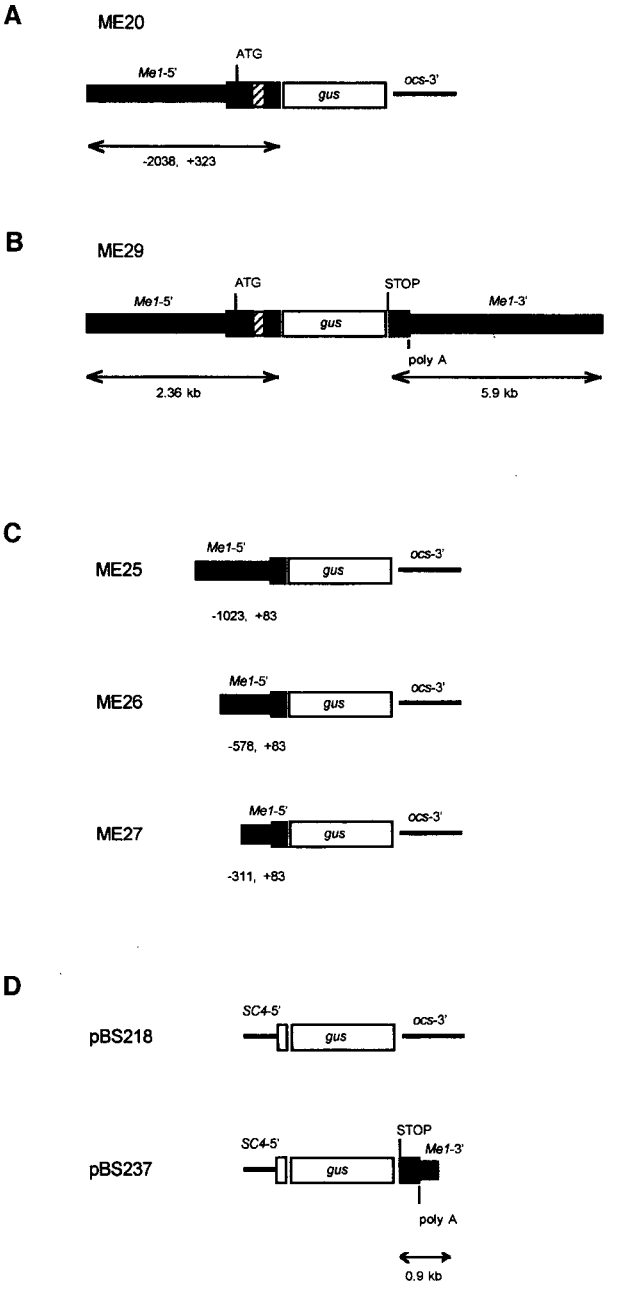

Figure 1. Chimeric *Me1–gus* Constructs Used in Plant Transformation.

(A) The ME20 construct with 2.36 kb of *ME1* 5′ fused to *gusA* with an *ocs* 3′ end. Exon 2 from *ME1* was fused in-frame to the *gusA* start codon.

(B) The ME29 construct with the same 5′ *ME1* sequences as ME20 but with 5.9 kb of the *ME1* 3′ end replacing the *ocs* 3′ fragment. The *ME1* 3′ fragment begins at the translation stop codon.

(C) Constructs containing deletions of *ME1* 5′. Transcriptional fusions were made that included the 5′ untranslated region of *ME1* and progressively shorter portions of *ME1* upstream DNA.

(D) Constructs used to determine whether *ME1* 3′ functions with a heterologous promoter. pBS218 contains 539 bp of the component 4 promoter of subterranean clover stunt virus (*SC4*-5′) fused to the same *gus–ocs* 3′ fragment as that used in ME20. In pBS237, the *ocs* 3′ fragment was replaced by 0.9 kb of *ME1* 3′ extending downstream from the translation stop codon.

Boxes indicate transcribed regions of *Me1*; exons are shown in black, and introns are diagonally striped. Thick lines indicate nontranscribed regions of *Me1*. Thin lines and open boxes indicate *gusA*, *ocs*, or *SC* sequences. Numbers indicate positions relative to the *ME1* start of transcription.

The 3′ Region of the *Me1* Gene Enhances GUS Expression in Leaves at Least 64-Fold

To determine quantitatively the relative levels of GUS activity present in leaves of ME20- and ME29-transformed plants, we measured GUS activity in extracts of leaves by using the fluorogenic GUS substrate 4-methylumbelliferyl β-D-glucuronide (Jefferson, 1987). As expected from the histochemical assays, GUS activity in leaf extracts from ME29-transformed plants was much higher than that measured for ME20-transformed plants (Table 1). The lowest expressing ME29-transformed plant exhibited 64 times as much GUS activity as the highest expressing ME20-transformed plant, whereas GUS activity in the highest expressing ME29-transformed plant was 440 times higher than that seen in the highest expressing ME20-transformed plant. Therefore, inclusion of the 3′ end of the *Me1* gene led to at least a 64-fold enhancement of GUS expression over the construct that included only the 5′ end of the *Me1* gene.

The 5′ Region of *Me1* Is Sufficient to Confer Bundle Sheath Preferential Expression on GUS

Because bundle sheath and mesophyll cells are intimately connected by a large number of plasmodesmata, which facilitate the movement of metabolites between the two cell types, it seemed possible that some or all of the histochemical staining seen in mesophyll cells could be the result of diffusion of the GUS reaction product from bundle sheath cells. Therefore, to obtain a more quantitative estimate of the distribution of GUS activity between the two main photosynthetic cell types in leaves of ME20- and ME29-transformed plants, we isolated mesophyll and bundle sheath cells and measured GUS activity in each cell fraction. The thick cell walls surrounding bundle sheath cells facilitate separation of the two cell types by differential homogenization. Two successive rounds of relatively gentle homogenization followed by filtration through a nylon mesh liberated fractions enriched in mesophyll cells. More complete homogenization of the material retained on the nylon mesh released a fraction of nearly pure bundle sheath strands consisting of veins surrounded by a ring of bundle sheath cells. Activities of the marker enzymes

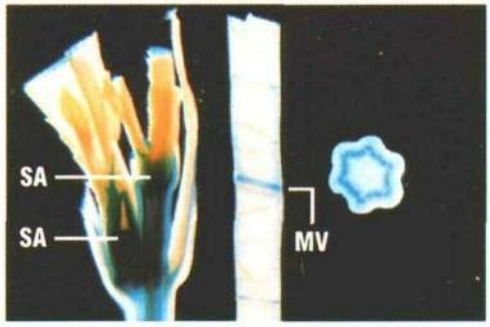

Figure 2. Histochemical Localization of GUS Activity in ME20-Transformed *F. bidentis*.

(Left) Shoot apex.
(Middle) Leaf section.
(Right) Transverse section of a stem.
All sections were taken from the same T_1 plant and were incubated overnight in X-gluc solution. SA, shoot apex; MV, midvein.

phosphoenolpyruvate carboxylase (PEPC; mesophyll specific) and NADP-ME (bundle sheath specific) were measured in each cell fraction to determine the degree of cross-contamination. These values were used to correct the measured GUS activities to obtain an accurate estimate of GUS activity per microgram of protein in each cell type (see Methods). Table 2 summarizes the measured enzyme activities and fraction purity for mesophyll cell and bundle sheath cell fractions from three plants transformed with ME20 and six plants transformed with ME29.

Figure 5 summarizes the distribution of GUS activity between mesophyll and bundle sheath cells in ME20- and ME29-transformed plants. GUS activity corrected for cross-contamination was higher in bundle sheath cells than in mesophyll cells in every plant analyzed, irrespective of the construct used to transform the plants. As shown in Table 3, the ratio of GUS activity in bundle sheath cells to that in mesophyll cells varied from 2.1 to 10.8, although one ME20-transformed plant had no detectable GUS activity in mesophyll cells. We conclude from these data that the 5′ region of *Me1* is sufficient to direct the preferential expression of GUS in bundle sheath cells and that inclusion of the 3′ region of *Me1* does not affect the distribution of GUS activity between the two cell types.

The 5′ and 3′ Regions of *Me1* Do Not Confer Significant Expression in the C_3 Plant Tobacco

To test whether the regulatory elements present in the 5′ and 3′ regions of *Me1* were active in C_3 plants, ME20 and ME29 were used to transform tobacco. This species was chosen because to date, no C_3 *Flaveria* species has been successfully transformed. At present, transformation systems are available only for C_4 (*F. bidentis*; Chitty et al., 1994) and C_3–C_4 (*F. pubescens*; Chu et al., 1997) *Flaveria* species.

Leaf, stem, and flower sections from six ME20- and 19 ME29-transformed tobacco plants were analyzed histochemically. In 21 of the plants, no blue color development was observed after overnight incubation. However, in two ME20-transformed plants and one ME29-transformed plant, some blue was detected in stem and leaf sections, but only in small

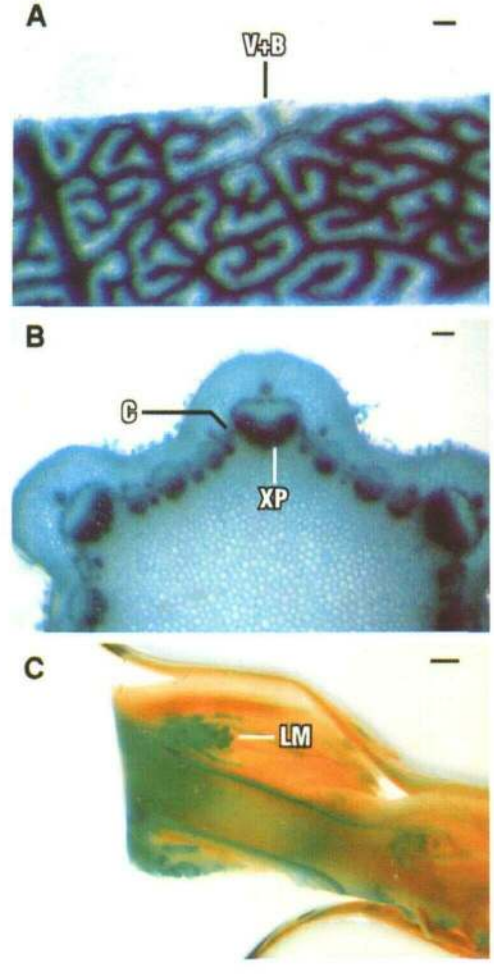

Figure 3. Histochemical Localization of GUS Activity in ME29-Transformed *F. bidentis*.

(A) Leaf section. Bar = 100 μm.
(B) Transverse section of a stem. Bar = 100 μm.
(C) Longitudinal section of a shoot apex. Bar = 1 mm.
All sections were taken from the same T_1 plant and were incubated for 4 hr in X-gluc solution. V+B, vein plus bundle sheath; C, cambium; XP, xylem parenchyma; LM, lateral meristem.

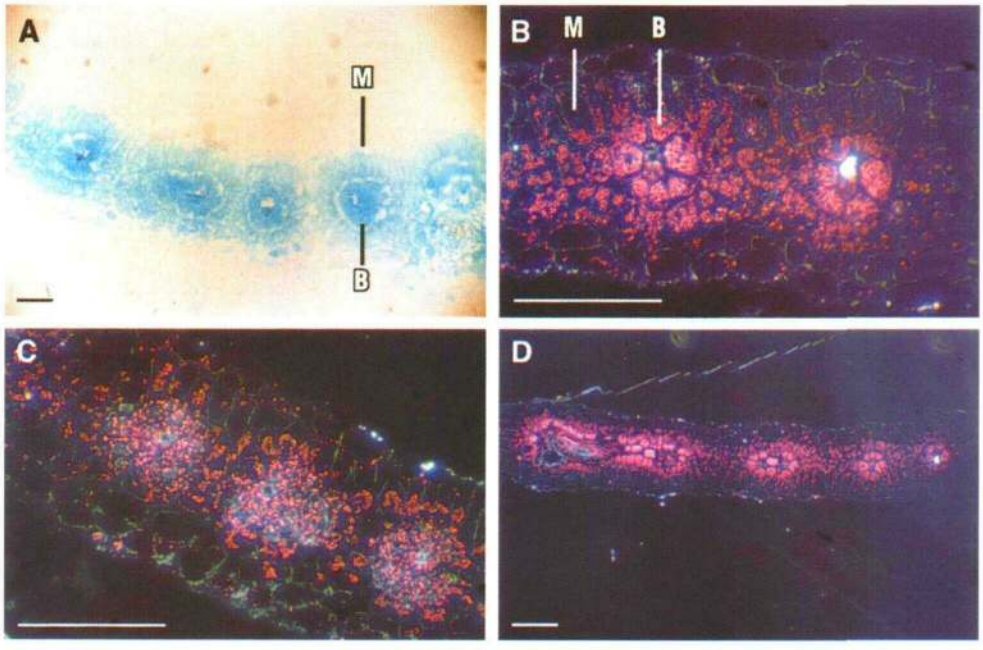

Figure 4. Fine-Scale Histochemical Localization of GUS Activity in Leaf Sections of ME29-Transformed *F. bidentis*.

(A) Bright-field view showing the concentration of the blue GUS product in bundle sheath cells.
(B) to **(D)** Dark-field views. Under dark-field illumination, the crystalline GUS product is visible as bright pink spots (Peleman et al., 1989). Sections were taken from the leaf shown in Figure 3A. M, mesophyll; B, bundle sheath. Bars in **(A)** to **(D)** = 100 μm.

patches. In addition, in one ME29-transformed plant, some blue color was observed in stigmas (data not shown). Biochemical assays of the selectable marker neomycin phosphotransferase were used to verify that all of the tobacco plants tested for GUS activity were transformed.

The 3′ Region of *Me1* Functions as an Efficient Terminator with a Heterologous Promoter

Having demonstrated the role of the 3′ region in *Me1* expression, we asked how the 3′ region would function in combination with a heterologous promoter. We selected the promoter of the component 4 gene of subterranean clover stunt virus, a multicomponent, single-stranded DNA virus (Boevink, 1995). This promoter has been shown to provide constitutive *gusA* gene expression at levels similar to the cauliflower mosaic virus 35S promoter in a number of dicotyledonous plants (B. Surin and P.M. Waterhouse, unpublished results). A chimeric construct was made in which a 539-bp fragment of virus component 4 (*SC4*) was fused upstream of *gusA*, which was followed by a 0.9-kb EcoRI fragment representing the region immediately downstream of the *Me1* stop codon (Figure 1D). For comparison, we also made a second construct in which the 0.9-kb *Me1* 3′ fragment was replaced by the *ocs* 3′ end, as was done in ME20 (Figure 1D). When introduced into *Nicotiana plumbaginifolia* protoplasts, similar levels of transient GUS expression were obtained with both constructs (Table 4). Stable transformation experiments

Table 1. GUS Activities in Extracts of Leaves from ME20- and ME29-Transformed Plants

Plant	Construct Used	Net GUS Activity (FU μg^{-1} protein hr^{-1})[a]
9A	ME20	27[b]
9B	ME20	27[b]
14A	ME20	17[b]
1A	ME29	5,730
1B	ME29	11,900
7A	ME29	10,600
7B	ME29	5,260
8A	ME29	1,720
8B	ME29	1,950

[a] FU, fluorescence unit.
[b] Corrected for background evolution of 4-methylumbelliferone (~8.3 FU hr^{-1}).

Table 2. Measured Marker Enzyme and GUS Activities for Mesophyll and Bundle Sheath Cell Fractions

Plant	Construct Used	Cell Fraction[a]	PEPC[b]	NADP-ME[c]	GUS (FU hr^{-1})[d]	Protein ($\mu g/\mu L$)	Fraction Purity[e] (%)
9A	ME20	MC1	272	45	10	0.23	61
		MC2	455	68	13	0.33	76
		BSC	12	394	64	0.77	99
9B	ME20	MC1	112	23	3.2	0.26	—[f]
		MC2	139	35	3.9	0.62	—[f]
		BSC	12	469	66	1.8	98
14A	ME20	MC1	75	26	3.9	0.14	82
		MC2	242	36	8.9	0.21	—[f]
		BSC	41	428	27	0.47	91
1A	ME29	MC1	45	15	474	0.08	73
		MC2	222	34	1,018	0.19	74
		BSC	26	281	3,970	0.43	94
1B	ME29	MC1	209	41	3,004	0.21	76
		MC2	381	67	4,515	0.30	71
		BSC	52	446	14,780	0.67	94
7A	ME29	MC1	238	39	1,882	0.19	77
		MC2	391	48	2,799	0.25	79
		BSC	69	348	9,864	0.4	91
7B	ME29	MC1	232	42	1,366	0.22	75
		MC2	162	65	2,163	0.33	76
		BSC	26	381	5,374	0.50	94
8A	ME29	MC1	180	27	162	0.15	87
		MC2	214	40	288	0.23	86
		BSC	22	480	1,655	0.40	95
8B	ME29	MC1	200	31	169	0.16	75
		MC2	360	57	340	0.23	68
		BSC	12	252	1,087	0.33	97

[a] MC1 and MC2 represent first and second mesophyll cell fractions, respectively. BSC represents the bundle sheath cell fraction.
[b] PEPC values represent $\Delta A_{340} \times 10^{-3}$ min^{-1}.
[c] NADP-ME values represent ΔA_{340} min^{-1}.
[d] FU, fluorescence unit.
[e] BSC purity represents the average of values obtained using MC1 or MC2 to calculate the proportion of protein deriving from MC versus BSC in each fraction.
[f] GUS activities in these mesophyll fractions were too low to permit accurate determination of fraction purity.

are under way to determine whether *Me1* 3′ sequences have an enhancing effect on heterologous promoters.

DISCUSSION

We have demonstrated that expression of the *F. bidentis Me1* gene, which encodes the isoform of NADP-ME utilized in C_4 photosynthesis, is regulated by elements both upstream and downstream of the coding region of the gene. These elements were shown to have distinct functions. The *Me1* downstream region was required for high-level expression in leaves but did not affect cell-type specificity. In contrast, the upstream region of the gene conferred bundle sheath cell preferential expression, even in the absence of the downstream element(s).

These findings indicate that regulation of *Me1* expression differs from that seen for other C_4 genes studied to date. In studies similar to ours, 5′ sequences from Flaveria genes encoding the C_4 isoforms of PEPC and pyruvate orthophosphate dikinase (PPDK) have been shown to be sufficient to direct high-level, mesophyll cell–specific expression of GUS in transgenic *F. bidentis* (Stockhaus et al., 1997; E. Rosche, J.A. Chitty, P. Westhoff, and W.C. Taylor, submitted manuscript). Similar conclusions have been reached for the maize genes encoding PPDK and the chlorophyll *a/b* binding protein of photosystem II by using transient expression assays (Matsuoka and Numazawa, 1991; Bansal and Bogorad, 1993). In none of these studies was the 3′ region of the gene in question tested for activity. Therefore, the possibility remains that downstream elements could also be involved in regulating mesophyll cell–specific gene expression. However, it seems unlikely that any downstream regulation of

these genes would be as quantitatively significant as that observed for *Me1*. It seems more likely that downstream elements do not play a major role in regulating the expression of mesophyll cell–specific genes. It will be interesting to determine whether other bundle sheath cell–specific genes also require sequences at their 3′ ends for expression.

Downstream elements have been implicated in the bundle sheath cell–specific expression of the small subunit of ribulose bisphosphate carboxylase (*RbcS*) in maize. Viret et al. (1994) have shown, using transient expression assays, that the 3′ region of the *RbcS-m3* gene is required to shift the balance of GUS expression from slightly mesophyll cell preferential to bundle sheath cell preferential. However, in contrast to the overall increase of leaf GUS activity conferred by the *Me1* 3′ region, Viret et al. (1994) found that the absolute level of GUS expression in bundle sheath cells was only slightly affected by the inclusion of the 3′ sequences. Their results indicate that the 3′ region of the *RbcS-m3* gene acts to suppress expression in mesophyll cells and therefore changes the proportion of expression in bundle sheath versus mesophyll cells.

Sequences at the 3′ end have been shown to contribute to the regulation of a number of other plant genes, both qualitatively and quantitatively (Thornburg et al., 1987; Dean et al., 1989; Dietrich et al., 1992; Larkin et al., 1993; Fu et al., 1995a, 1995b). In several of these examples, the 3′ sequences are required for correct spatial patterning of gene expression (Dietrich et al., 1992; Larkin et al., 1993; Fu et al., 1995a), and in one case, 3′ sequences are required for wound-inducible expression (Thornburg et al., 1987). These results are in contrast with our finding that the *Me1* 3′ fragment appears to act primarily by increasing the level of GUS expression and does not alter its cell specificity. Quantitative regulation of two petunia *RbcS* genes is accomplished by sequences at both the 5′ and 3′ ends (Dean et al., 1989).

The precise mode of action of the downstream region of *Me1* remains to be elucidated. The *gusA–ocs* 3′ fragment combination results in high-level GUS activity in Flaveria leaves when driven by 5′ sequences from the *F. trinervia Pdk* gene, which encodes PPDK (E. Rosche, J.A. Chitty, P. Westhoff, and W.C. Taylor, submitted manuscript), as well as by the cauliflower mosaic virus 35S promoter (Chitty et al., 1994), indicating that the *ocs* 3′ end functions as an efficient terminator and 3′ untranslated region in Flaveria. Additional experiments are under way to determine whether the *Me1* 3′ fragment affects transcription, mRNA turnover, or translation.

Another possible explanation for low GUS expression seen in leaves of ME20-transformed plants is that a negative regulatory element is present in the 5′ region of *Me1*, and relief from the negative effects of this element requires downstream *Me1* sequences. However, analysis of the 5′ deletion

Table 3. Ratios of GUS Activity Present in Bundle Sheath Cells to Mesophyll Cells

Plant	Construct Used	Cell Fraction	GUS_{BSC}/GUC_{MC}[a]
9A	ME20	MC1	4.5
		MC2	8.0
9B	ME20	MC1	—[b]
		MC2	—[b]
14A	ME20	MC1	3.0
		MC2	—[b]
1A	ME29	MC1	2.1
		MC2	2.4
1B	ME29	MC1	2.4
		MC2	2.3
7A	ME29	MC1	4.6
		MC2	3.4
7B	ME29	MC1	2.4
		MC2	2.2
8A	ME29	MC1	8.1
		MC2	5.7
8B	ME29	MC1	10.8
		MC2	5.7

[a] Ratios represent net GUS activity per unit of protein calculated for bundle sheath cells (GUS_{BSC}) divided by that for the indicated mesophyll cell fraction (GUS_{MC}).
[b] GUS activities in these mesophyll fractions were too low to permit accurate determination of the fraction of cross-contamination.

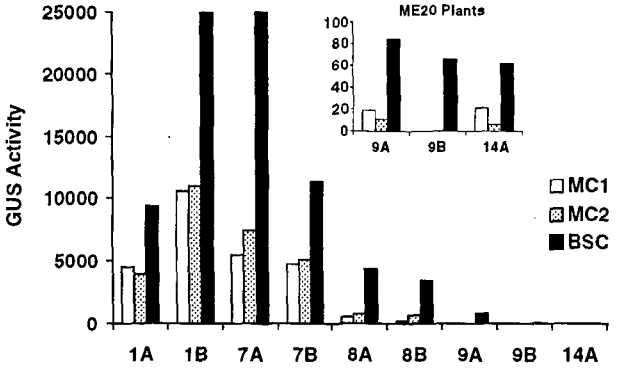

Figure 5. Expression of GUS in Mesophyll and Bundle Sheath Cell Fractions from Leaves of Six Different ME29- and Three Different ME20-Transformed *F. bidentis* Plants.

GUS activities were corrected for fraction cross-contamination and expressed as fluorescence units per microgram of protein per hour. MC1 and MC2 denote first and second mesophyll cell fractions, respectively. BSC denotes the bundle sheath cell fraction. Plants 1A, 1B, 7A, 7B, 8A, and 8B were transformed with ME29. Plants 9A, 9B, and 14A were transformed with ME20. The inset shows GUS activity in ME20-transformed plants with the vertical axis expanded. For ME20-transformed plants, the background evolution of 4-methylumbelliferone (~8.3 fluorescence units hr^{-1}) was subtracted before the calculation of cell-type distribution of GUS activity. GUS activities in both mesophyll cell fractions of plant 9B and the MC2 fraction of plant 14A were too low to determine cell-type distribution accurately.

Table 4. Transient GUS Expression Driven by a Heterologous Promoter with the *Me1* 3′ Fragment in *N. plumbaginifolia* Protoplasts

	GUS Activity (pmol mg^{-1} protein min^{-1})[a]	
Construct	Experiment 1	Experiment 2
pBS218 (*ocs* 3′)	75	56
pBS237 (*Me1* 3′)	117	122

[a] Each value represents the average of duplicate transient expression assays.

constructs ME25, ME26, and ME27 argue against the possibility of such a negative regulatory element >0.39 kb upstream of the *Me1* start codon or within the first exon or first intron.

The 5′ region of *Me1* was found to be sufficient to direct bundle sheath cell–preferential expression of GUS with either the *Me1* 3′ or *ocs* 3′ fragment. It is conceivable that this expression pattern could be a reflection of some nonspecific reduction of transgene expression in mesophyll cells relative to bundle sheath cells. However, *F. bidentis* plants transformed with the construct 35S–*gusA*–*ocs* 3′ show high levels of GUS activity in both cell types (cf. Figure 3A with Figure 2 in Chitty et al. [1994]), and *F. bidentis* plants transformed with *PpcA1–gusA* (which utilizes the promoter from the *F. trinervia* gene encoding the C_4 isoform of PEPC) show high-level GUS activity specifically in mesophyll cells (Stockhaus et al., 1997). Therefore, it appears that the cell preferential expression seen in ME20- and ME29-transformed plants is a specific result of inclusion of the 5′ region of *ME1*.

It is interesting that the *Me1* 5′ region confers only two- to 10-fold higher expression in bundle sheath cells than in mesophyll cells. This degree of cell preference is lower than would be expected from the strict localization of NADP-ME in bundle sheath cells of *F. bidentis* (Meister et al., 1996). It is possible that other mechanisms may be involved in fine-tuning the cell-specific expression of NADP-ME. For instance, post-transcriptional events may influence cell specificity, as has been seen with other C_4 species. In the C_4 dicot *Amaranthus hypochondriacus*, transcription and translation of some genes involved in C_4 photosynthesis are not coupled at all developmental stages (Wang et al., 1992, 1993a; Boinski et al., 1993; Ramsperger et al., 1996). Similar processes, relying on sequences within the *Me1* coding region, may help to control bundle sheath cell specificity. Another possibility is that transcription of *Me1* is regulated in part by sequences outside of the regions studied. Such sequences could lie further upstream (or downstream, but this seems less likely) or could be within the exons and/or introns of *Me1*.

We were also interested to find that promoter elements present in ME29, which were sufficient to confer high-level expression in Flaveria leaves, were inactive in tobacco leaves. This is in contrast with a previous report in which the *F. trinervia PpcA1* promoter conferred high-level leaf expression on *gusA* in transgenic tobacco (Stockhaus et al., 1994). This activity was found preferentially in the palisade parenchyma. In addition, 5′ sequences of maize genes encoding PPDK, PEPC, and the small subunit of ribulose bisphosphate carboxylase have been shown to drive detectable expression in leaves of transgenic tobacco (Matsuoka and Sanada, 1991). These three promoters are also active in transgenic rice, leading to high-level, mesophyll cell–specific expression (Matsuoka et al., 1993, 1994). Taken together, these results indicate that leaf-specific expression of *Me1* may rely on C_4-specific positive regulatory elements, whereas expression of the other genes mentioned above uses factors that are also present in C_3 plants. One simple possibility is that the apparent downstream enhancer-like element present in *Me1* interacts with C_4-specific *trans*-acting factors, leading to high-level expression in leaves. The absence of such factors in tobacco might lead to the observed lack of GUS activity in this C_3 plant.

GUS expression in stems and apices was controlled by the *Me1* upstream region alone. High-level GUS activity in stems was found in the cambium and in parenchyma cells associated with phloem and xylem. It may be significant that these are the cells with the greatest number of chloroplasts. Although these cells are potentially active in photosynthesis, the absence of any C_4 cellular differentiation suggests that the C_3 pathway probably operates in stems. Therefore, it is curious that the promoter of a C_4 gene is highly active in these cells. The *F. trinervia Pdk* promoter also directs a similar pattern of GUS expression in stems (E. Rosche, J. Chitty, P. Westhoff, and W.C. Taylor, submitted manuscript). It is possible that GUS expression in stems and apices is not a true indication of the expression pattern of the *Me1* and *Pdk* genes but is due to the absence in the constructs of *cis*-acting sequences responsible for suppressing nonleaf expression. Conversely, Berry and colleagues have demonstrated that several C_4 genes are expressed in meristems and leaf primordia in amaranth (Ramsperger et al., 1996), indicating that at least part of the non-leaf-associated GUS activity observed in *F. bidentis* transformants may reflect actual expression of *Me1*.

The work presented here provides a range of interesting avenues for additional experiments. Of primary interest to us is finer scale mapping of both the 5′ and 3′ regions of *Me1* to more precisely determine the location of the *cis* regulatory elements involved in high-level bundle sheath cell–specific expression. Experiments in which smaller fragments of both ends of *Me1* are linked to GUS are in progress. In addition, we are interested in characterizing the nature of the downstream putative enhancer-like element. To this end, the *Me1* 3′ region is being analyzed in different positions relative to *gusA* and in conjunction with other promoters. Finally, we are interested in determining the mechanism by which cell-specific gene expression is determined. Some obvious possibilities include suppression of expression in mesophyll cells, the enhancement of expression in bundle sheath cells,

or a combination of these two. It seems likely, based on studies of C_4 gene expression in other species (Sheen, 1990; Matsuoka and Numazawa, 1991; Bansal et al., 1992; Bansal and Bogorad, 1993; Wang et al., 1993b; Viret et al., 1994; Purcell et al., 1995; Ramsperger et al., 1996), that cell-specific expression involves a complex interplay between a number of different factors, including developmental stage, metabolic status, environmental signals, and cell type.

METHODS

Construction of Chimeric Genes for Transformation

For construction of ME20, a 3.5-kb BamHI-XhoI fragment of pKIWI101 (Janssen and Gardner, 1989) containing the β-glucuronidase *gusA* gene and octopine synthase (*ocs*) 3′ terminator was excised and ligated into BamHI-SalI–cut pUC18. This construct was then cut with BamHI plus SalI, and a 2.2-kb BamHI-XhoI fragment from the 5′ region of the *Flaveria bidentis Me1* gene (Marshall et al., 1996) was ligated in-frame to the 5′ end of the *gusA* gene. The resulting plasmid was cut with HindIII and ligated into the binary vector pGA470 (An et al., 1985), which was also cut with HindIII.

For construction of ME29, the 2.2-kb 5′ BamHI-XhoI fragment of *Me1* used in the construction of ME20 was ligated to the 5′ end of a 1.9-kb SalI-EcoRI fragment of pKIWI101 (Janssen and Gardner, 1989) containing the *gusA* gene. The chimeric *Me1–gusA* insert from this construct was excised with HindIII plus EcoRI and ligated to the 5′ end of a 5-kb EcoRI-SacI fragment from the 3′ end of *Me1* (beginning ~0.9 kb downstream of the *Me1* stop codon). The 0.9-kb *Me1* fragment from the stop codon to the 5′ end of the 5-kb EcoRI-SacI fragment was synthesized by polymerase chain reaction (PCR), using a 5′ primer containing a synthetic EcoRI linker: 5′-CCGAATTCGTTT-AGCGGGGGAAAAAGGACAG-3′. This primer was designed from the sequence immediately downstream of the *F. bidentis Me1* stop codon (Marshall et al., 1996). A 4-kb EcoRI subclone of ME7 (Marshall et al., 1996) containing the region of interest was used as a template, with the above-mentioned *Me1*-specific primer and the M13 −21 primer. The resulting PCR product was cut with EcoRI and ligated into the EcoRI site separating the *gusA* gene and the 5-kb 3′ fragment from *Me1*. This ligation resulted in the reconstruction of the 3′ region of *Me1* from the stop codon extending 5.9 kb downstream. This construct was linearized with KpnI and ligated into KpnI-cut pGA482 (An, 1987).

The three 5′ deletion constructs were made by first generating exonuclease III deletions of the BamHI-XhoI *Me1* 5′ fragment. The deletion constructs were then amplified by PCR using a 5′ primer from pUC18 containing a synthetic HindIII site (CCAAGCTTGTAAAAC-GACGGCCAGT) and a 3′ primer that hybridizes immediately upstream of the start codon of *Me1* and containing an artificial PstI site (CCCTGCAGGGTGCGAGAGAAGAGTGTGAATT). The PCR products were cut with HindIII plus PstI and cloned upstream of the *gusA–ocs* 3′ sequences from pKIWI101. The resulting plasmid was linearized with HindIII and cloned into pGA470.

The *SC4* promoter of subterranean clover stunt virus was cloned by PCR amplification of a 539-bp region upstream of the component 4 coding region, using primers to introduce BamHI and NcoI restriction sites (Boevink, 1995). The BamHI-NcoI fragment was blunt ended with the Klenow fragment of DNA polymerase I and then ligated to the *gusA–ocs* 3′ sequences from pKIWI101 at the filled-in SalI site to make construct pBS218. In a second construct, pBS237, the *ocs* 3′ end was replaced by the 0.9-kb *Me1* 3′ EcoRI PCR fragment extending downstream from the translation stop codon.

Plant Transformation

Chimeric gene constructs in binary vectors were introduced into *Agrobacterium tumefaciens* and used to transform *F. bidentis* hypocotyls, as described by Chitty et al. (1994). All transgenic *F. bidentis* plants analyzed were progeny of self-pollinated primary transformants. Tobacco was transformed using standard procedures, and transformation was verified by assaying the selectable marker neomycin phosphotransferase.

Transient β-glucuronidase (GUS) expression of constructs pBS218 and pBS237 was measured in *Nicotiana plumbaginifolia* protoplasts, as described by Graham and Larkin (1995).

Histochemical Localization of GUS Activity

Plant material was immersed in 50 mM sodium-phosphate buffer, pH 7.0, and cut into 1- to 2-mm sections. The sections were then incubated in 50 mM sodium-phosphate, pH 7.0, 0.5 mM potassium ferricyanide, 0.5 mM potassium ferrocyanide, and 1 mM 5-bromo-4-chloro-3-indolyl β-D-glucuronide (X-gluc) at 37°C. For fine-scale analysis of GUS expression, histochemically stained material was fixed in 3% glutaraldehyde and embedded in LR White resin (London Resin Company, Basingstoke, UK), cut into 1- to 5-μm thick sections, and observed using dark-field illumination.

Cell Separation Experiments and Enzyme Assays

Preparations of mesophyll and bundle sheath cells were made using a modification of the method of Meister et al. (1996). Young leaves from greenhouse-grown progeny of selfed *F. bidentis* primary transformants were deribbed and chopped with a razor blade. Chopped leaves were suspended in 70 mL of buffer A (0.3 M sorbitol, 25 mM Pipes, pH 7.4, 10 mM DTT, and 1 mM $MgCl_2$) and homogenized for 5 sec at low speed (setting 2) in a Sorvall Omnimixer (Du Pont, Newtown, CT). An aliquot representing unfractionated leaves was removed and homogenized in a tissue homogenizer (Glas-Col, Terre Haute, IN). A second aliquot, representing mesophyll cells, was removed and filtered through a 20-μm nylon mesh, and the filtrate was homogenized in a Dounce tissue homogenizer. The remaining (unfiltered) material was homogenized for an additional 5 sec at low speed, and a second mesophyll cell sample was removed, filtered, and homogenized as described above. Finally, the remainder was homogenized for 40 sec at full speed in the Omnimixer and filtered through a 20-μm nylon mesh. The material retained on the mesh (representing bundle sheath strands) was washed with 20 mL of buffer A, then suspended in 20 mL of buffer B (50 mM Pipes, pH 7.0, 10 mM $MgCl_2$, 0.5 mM EDTA, 1% PVP, 5 mM DTT, 2 mM phenylmethylsulfonyl fluoride, and 2 mM ε-amino-*n*-caproic acid), and homogenized in a Dounce tissue homogenizer. Aliquots of all fractions were removed for protein determination using the Bio-Rad protein assay reagent with BSA as standard, and the remainder of each fraction was adjusted to 0.1% (w/v) BSA and frozen in liquid N_2. Samples were stored at −80°C until assayed.

Marker enzyme (phosphoenolpyruvate carboxylase [PEPC] and NADP–malic enzyme [NADP-ME]) activities were measured using a modification of the protocols described by Ashton et al. (1990). PEPC activity was assayed in 1 mL of solution containing 25 mM *N*-tris(hydroxymethyl)methylglycine–KOH, pH 8.3, 5 mM $MgSO_4$, 5 mM $KHCO_3$, 5 mM phosphoenolpyruvate, 4 mM DTT, 0.25 mM NADH, 1 mM glucose 6-phosphate, and 2 units of malate dehydrogenase. NADP-ME was assayed in 1 mL of solution containing 25 mM *N*-tris(hydroxymethyl)methylglycine–KOH, pH 8.3, 5 mM malate, 2 mM $MgCl_2$, 0.5 mM NADP, and 0.2 mM EDTA.

GUS activity in leaf fractions was measured using the fluorogenic GUS substrate 4-methylumbelliferyl β-D-glucuronide, as described by Jefferson (1987). Fluorescence was measured in a spectrofluorometer (SLM Instruments, Urbana, IL). Reactions were incubated for 24 hr at 37°C, and aliquots were removed after 0.2, 2, 5, 8, and 24 hr. Fluorescence values were plotted versus incubation time, and the initial reaction rate was determined using nonlinear regression.

Calculation of Levels of GUS Expression in Mesophyll and Bundle Sheath Fractions

Net GUS activity present in mesophyll and bundle sheath cell fractions was calculated using an iterative process with the following assumptions:

(1) for any fraction, $GUS_{Total} = GUS_{MC} + GUS_{BSC}$,
(2) GUS_{MC}/PEPC is constant, and
(3) GUS_{BSC}/ME is constant,

where GUS_{Total} is the measured GUS activity for the fraction, GUS_{MC} is the portion of GUS_{Total} derived from mesophyll cells, GUS_{BSC} is the portion of GUS_{Total} derived from bundle sheath cells, PEPC is the measured PEPC activity, and ME is the measured NADP-ME activity. Rates of activity were used for all enzymes. As an initial approximation, it was assumed that for mesophyll fractions, $GUS_{Total} = GUS_{MC}$. Using this approximation and the measured PEPC activities for each fraction, a maximum value for GUS_{MC} and a minimum value for GUS_{BSC} present in the bundle sheath cell fraction were calculated:

$$\text{maximum } GUS_{MC}^{BSC} = [GUS_{MC}^{MC} \div PEPC^{MC}] \times PEPC^{BSC}$$

$$\text{minimum } GUS_{BSC}^{BSC} = GUS_{Total}^{BSC} - \text{maximum } GUS_{MC}^{BSC}$$

where superscripts denote the cell fraction in which the activity was measured and subscripts denote the cell type from which the activity derived. The latter number was then used with the ME activities measured in each fraction to determine a minimum value for GUS_{BSC} and a maximum value for GUS_{MC} present in the mesophyll fraction:

$$\text{minimum } GUS_{BSC}^{MC} = [GUS_{BSC}^{BSC} \div ME^{BSC}] \times ME^{MC}$$

$$\text{maximum } GUS_{MC}^{MC} = GUS_{Total}^{MC} - \text{minimum } GUS_{BSC}^{MC}$$

The process was reiterated using this refined value for GUS_{MC} in the mesophyll fraction. Iteration was continued until constant values were obtained for GUS_{MC} in mesophyll and GUS_{BSC} in bundle sheath cells.

To obtain values for GUS activity per unit of protein, $Protein_{MC}$ and $Protein_{BSC}$ values were calculated for each fraction following the same iterative procedure. GUS activity per unit of protein was defined as $GUS_{MC}/Protein_{MC}$ for mesophyll fractions and $GUS_{BSC}/Protein_{BSC}$ for bundle sheath cell fractions. Purity of fractions was calculated as $Protein_{MC}/Protein_{Total}$ for mesophyll fractions and $Protein_{BSC}/Protein_{Total}$ for bundle sheath cell fractions.

ACKNOWLEDGMENTS

We thank Stuart Craig, Celia Miller, and Margaret McCully for help and advice with microscopic analyses, Phil Larkin for protoplast transformations, Elke Rosche for help with the cell separations, Mandy Watson for technical assistance, and Ian Watson for help with the figures. We thank Elke Rosche and Rudy Dolferus for comments on the manuscript.

Received March 17, 1997; accepted June 17, 1997.

REFERENCES

An, G. (1987). Binary Ti vectors for plant transformation and promoter analysis. Methods Enzymol. **153,** 292–305.

An, G., Watson, B.D., Stachel, S., Gordon, M.P., and Nester, E.W. (1985). New cloning vehicles for transformation of higher plants. EMBO J. **4,** 277–284.

Ashton, A.R., Burnell, J.N., Furbank, R.T., Jenkins, C.L.D., and Hatch, M.D. (1990). Enzymes of C_4 photosynthesis. In Methods in Plant Biochemistry, Vol. 3, P.J. Lea, ed (London: Academic Press), pp. 39–72.

Bansal, K.C., and Bogorad, L. (1993). Cell type–preferred expression of maize *cab*-m1: Repression in bundle sheath cells and enhancement in mesophyll cells. Proc. Natl. Acad. Sci. USA **90,** 4057–4061.

Bansal, K.C., Viret, J.-F., Haley, J., Khan, B.M., Schantz, R., and Bogorad, L. (1992). Transient expression from *cab-m1* and *rbcS-m3* promoter sequences is different in mesophyll and bundle sheath cells in maize leaves. Proc. Natl. Acad. Sci. USA **89,** 3654–3658.

Boevink, P. (1995). Molecular Characterisation of Subterranean Clover Stunt Virus. PhD Dissertation (Canberra: Australian National University).

Boinski, J.J., Wang, J.-L., Xu, P., Hotchkiss, T., and Berry, J.O. (1993). Post-transcriptional control of cell type–specific gene expression in bundle sheath and mesophyll chloroplasts of *Amaranthus hypochondriacus*. Plant Mol. Biol. **22,** 397–410.

Chitty, J.A., Furbank, R.T., Marshall, J.S., Chen, Z., and Taylor, W.C. (1994). Genetic transformation of the C_4 plant, *Flaveria bidentis*. Plant J. **6,** 949–956.

Chu, C.C., Qu, N., Bassüner, B., and Bauwe, H. (1997). Genetic transformation of the C_3–C_4 intermediate species, *Flaveria pubescens* (Asteraceae). Plant Cell Rep. **16,** 715–718.

Dean, C., Favreau, M., Bond-Nutter, D., Bedbrook, J., and Dunsmuir, P. (1989). Sequences downstream of translation start regulate quantitative expression of two petunia *rbcS* genes. Plant Cell **1,** 201–208.

Dietrich, R.A., Radke, S.E., and Harada, J.J. (1992). Downstream DNA sequences are required to activate a gene expressed in the root cortex of embryos and seedlings. Plant Cell **4,** 1371–1382.

Fu, H., Kim, S.Y., and Park, W.D. (1995a). High-level tuber expression and sucrose inducibility of a potato *Sus4* sucrose synthase gene require 5′ and 3′ flanking sequences and the leader intron. Plant Cell **7,** 1387–1394.

Fu, H., Kim, S.Y., and Park, W.D. (1995b). A potato *Sus3* sucrose synthase gene contains a context-dependent 3′ element and a leader intron with both positive and negative tissue-specific effects. Plant Cell **7,** 1395–1403.

Furbank, R.T., and Taylor, W.C. (1995). Regulation of photosynthesis in C_3 and C_4 plants: A molecular approach. Plant Cell **7,** 797–807.

Graham, M.W., and Larkin, P.J. (1995). Adenine methylation at dam sites increases transient gene expression in plant cells. Transgen. Res. **4,** 324–331.

Hatch, M.D. (1987). C_4 photosynthesis: A unique blend of modified biochemistry, anatomy and ultrastructure. Biochim. Biophys. Acta **895,** 81–106.

Janssen, B.-J., and Gardner, R.C. (1989). Localized transient expression of GUS in leaf discs following cocultivation with *Agrobacterium*. Plant Mol. Biol. **14,** 61–72.

Jefferson, R. (1987). Assaying chimeric genes in plants: The GUS gene fusion system. Plant Mol. Biol. Rep. **5,** 387–405.

Larkin, J.C., Oppenheimer, D.G., Pollock, S., and Marks, M.D. (1993). Arabidopsis *GLABROUS1* gene requires downstream sequences for function. Plant Cell **5,** 1739–1748.

Marshall, J.S., Stubbs, J.D., and Taylor, W.C. (1996). Two genes encode highly similar chloroplastic NADP-malic enzymes in *Flaveria.* Plant Physiol. **111,** 1251–1261.

Matsuoka, M., and Numazawa, T. (1991). *cis*-Acting elements in the pyruvate, orthophosphate dikinase gene from maize. Mol. Gen. Genet. **228,** 143–152.

Matsuoka, M., and Sanada, Y. (1991). Expression of photosynthetic genes from the C_4 plant, maize, in tobacco. Mol. Gen. Genet. **225,** 411–419.

Matsuoka, M., Tada, Y., Fujimura, T., and Kano-Murakami, Y. (1993). Tissue-specific light-regulated expression directed by the promoter of a C_4 gene, maize pyruvate, orthophosphate dikinase, in a C_3 plant, rice. Proc. Natl. Acad. Sci. USA **90,** 9586–9590.

Matsuoka, M., Kyozuka, J., Shimamoto, K., and Kano-Murakami, Y. (1994). The promoters of two carboxylases in a C_4 plant (maize) direct cell-specific, light-regulated expression in a C_3 plant (rice). Plant J. **6,** 311–319.

Meister, M., Agostino, A., and Hatch, M.D. (1996). The roles of malate and aspartate in C_4 photosynthetic metabolism of *Flaveria bidentis* (L.). Planta **199,** 262–269.

Peleman, J., Boerjan, W., Engler, G., Seurink, J., Botterman, J., Alliotte, T., Van Montagu, M., and Inzé, D. (1989). Strong cellular preference in the expression of a housekeeping gene of *Arabidopsis thaliana* encoding *S*-adenosylmethionine synthetase. Plant Cell **1,** 81–93.

Purcell, M., Mabrouk, Y.M., and Bogorad, L. (1995). Red/far-red and blue light-responsive regions of maize *rbcS*-m3 are active in bundle sheath and mesophyll cells, respectively. Proc. Natl. Acad. Sci. USA **92,** 11504–11508.

Ramsperger, V.C., Summers, R.G., and Berry, J.O. (1996). Photosynthetic gene expression in meristems and during initial leaf development in a C_4 dicotyledonous plant. Plant Physiol. **111,** 999–1010.

Sheen, J. (1990). Metabolic repression of transcription in higher plants. Plant Cell **2,** 1027–1038.

Sheen, J. (1991). Molecular mechanisms underlying the differential expression of maize pyruvate, orthophosphate dikinase genes. Plant Cell **3,** 225–245.

Stockhaus, J., Poetsch, W., Steinmüller, K., and Westhoff, P. (1994). Evolution of the C_4 phosphoenolpyruvate carboxylase promoter of the C_4 dicot *Flaveria trinervia*: An expression analysis in the C_3 plant tobacco. Mol. Gen. Genet. **245,** 286–293.

Stockhaus, J., Schlue, U., Koczor, M., Chitty, J.A., Taylor, W.C., and Westhoff, P. (1997). The promoter of the gene encoding the C_4 form of phosphoenolpyruvate carboxylase directs mesophyll-specific expression in transgenic C_4 *Flaveria* spp. Plant Cell **9,** 479–489.

Thornburg, R.W., An, G., Cleveland, T.E., Johnson, R., and Ryan, C.A. (1987). Wound-inducible expression of a potato inhibitor II–chloramphenicol acetyltransferase gene fusion in transgenic potato plants. Proc. Natl. Acad. Sci. USA **84,** 744–748.

Viret, J.-F., Mabrouk, Y., and Bogorad, L. (1994). Transcriptional photoregulation of cell-type-preferred expression of maize *rbcS*-m3: 3′ and 5′ sequences are involved. Proc. Natl. Acad. Sci. USA **91,** 8577–8581.

Wang, J.-L., Klessig, D.F., and Berry, J.O. (1992). Regulation of C_4 gene expression in developing amaranth leaves. Plant Cell **4,** 173–184.

Wang, J.-L., Long, J.J., Hotchkiss, T., and Berry, J.O. (1993a). C_4 photosynthetic gene expression in light- and dark-grown amaranth cotyledons. Plant Physiol. **102,** 1085–1093.

Wang, J.-L., Turgeon, R., Carr, J.P., and Berry, J.O. (1993b). Carbon sink-to-source transition is coordinated with establishment of cell-specific gene expression in a C_4 plant. Plant Cell **5,** 289–296.